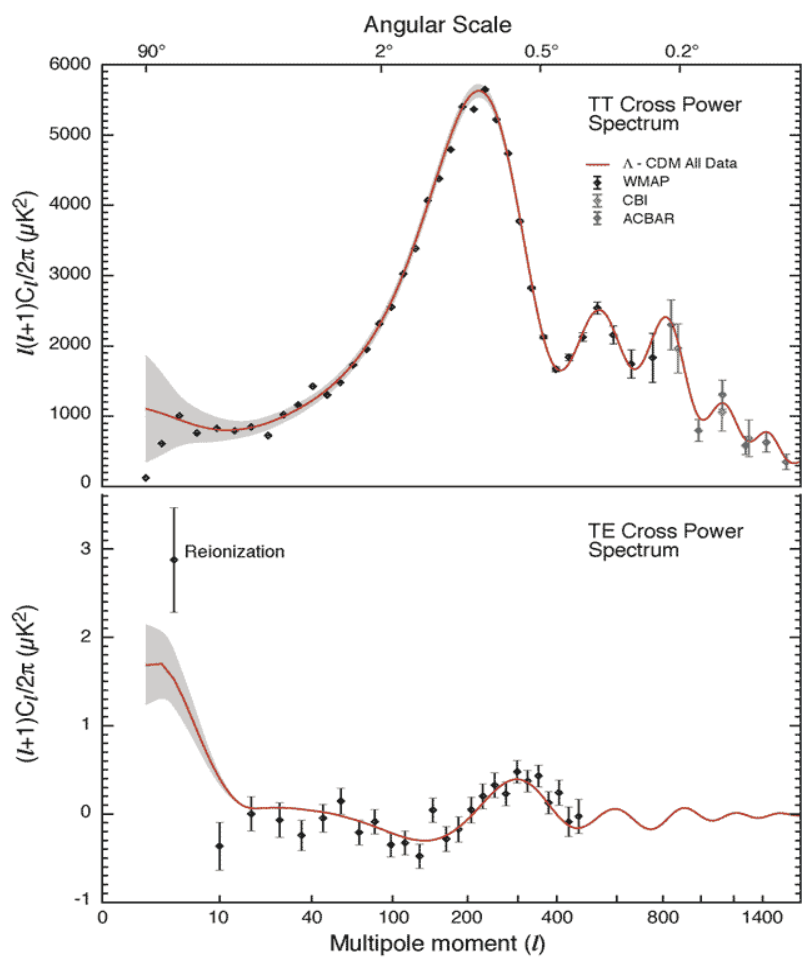


6. Cosmic Microwave Background

6.1 Overview

We now come to the point to explain the temperature anisotropy in the CMB (upper panel of the plot). The CMB is decomposed in spherical harmonics (l -space). Let us denote the time, when a typical photon was last scattered (i.e. around recombination) by η_* . Our time coordinate is η_0 , so the comoving distance to the last scattering surface is $\eta_0 - \eta_*$. A certain length scale ℓ^* therefore subtends in the CMB an angle $\vartheta = \frac{1}{k(\eta_0 - \eta_*)}$. For sufficiently large l , we can roughly identify ϑ with $\frac{1}{\ell}$. We have seen already (indirectly) that the tightly coupled baryon-photon fluid oscillates. The CMB therefore gives a snapshot of the oscillation phase of the particular k -modes at the time η_* . Another apparent feature is, though, the damping of modes with large l . This can be understood when noting that the mean free path of a photon is $\lambda_{MFP} = \frac{1}{n_e \sigma_T}$, where n_e is the number density of electrons. The number density scales as a^{-3} , whereas the Hubble rate



as $a^{-\frac{3}{2}}$ during matter domination. Hence, the tight coupling approximation is at early times more justified than at late times. The freely streaming photons tend to erase the perturbations on scales smaller than the diffusion scale

$$\lambda_D \sim \lambda_{MFP} \sqrt{n_e \sigma_T H^{-1}}, \text{ where}$$

the discriminant counts the number of scatterings in a Hubble time and we use the fact that the distance covered by a random walk is proportional to the square root of the number of steps.

6.2 Large-Scale Anisotropies

From the last chapter, we recall that on super-horizon scales, $\dot{\Phi}' = -\dot{\phi}'$, such that $\Phi_0 = -\dot{\phi} + \text{const.}$ (the Eqs. hold for both, photons and neutrinos). On the other hand, we found that the initial condition is $\Phi_0 = \frac{\dot{\phi}}{2}$, such that the constant is $\frac{3}{2}\dot{\phi}_p$.

We have also found for the large-scale evolution of $\dot{\Phi}$ that

$$\dot{\Phi} = \dot{\Phi}(0) \frac{1}{10g^3} (16\sqrt{1+g} + 9g^3 + 2g^2 - 8g - 16) \xrightarrow{g \gg 1} \frac{9}{10} \dot{\Phi}(0)$$

We therefore find that

$$\Phi_0(k, \gamma_*) = -\dot{\Phi}(k, \gamma_*) + \frac{3}{2} \dot{\Phi}_p(k) = \frac{2}{3} \dot{\Phi}(k, \gamma_*)$$

$$-1 + \frac{3}{2} \frac{70}{9} = -1 + \frac{5}{3} = \frac{2}{3}$$

Photon Diffusion

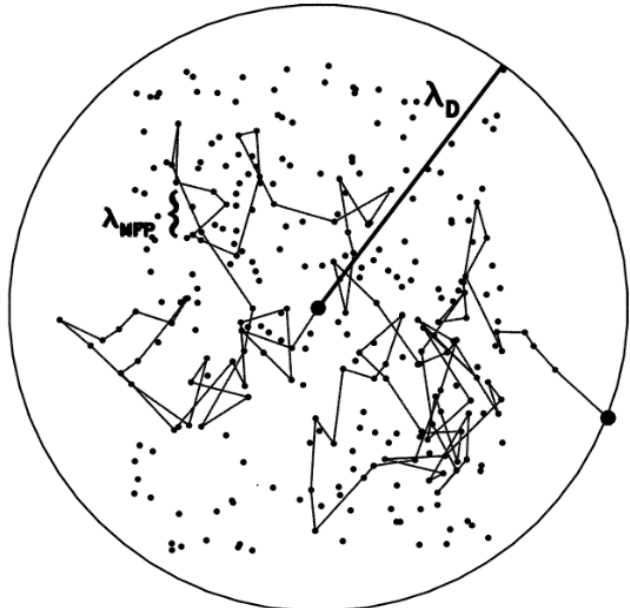


Figure 8.3. Photon diffusion through the electron gas. Electrons are denoted as points. Shown is a typical photon path as it scatters off electrons. The mean free path is λ_{MFP} . After a Hubble time, the photon has scattered many times, so that it has moved a distance of order λ_D .

Below, we see that the temperature observed today is given by $\Theta_0 + \Psi$, as the photons need to climb out of potential wells. Using further that $\bar{\Phi} \approx -\Psi$, we find

$$(\Theta_0 + \Psi)(k, \eta_*) = \frac{1}{3} \Psi(k, \eta_*)$$

We can also relate the observed temperature perturbations to the Dark Matter overdensity. For this purpose, note that we found the initial condition for adiabatic perturbations

$$\delta = 3\Theta_0 = \frac{3}{2} \bar{\Phi}$$

The large-scale evolution is governed by $\delta' = -3\bar{\Phi}'$, which we can integrate given above boundary condition to

$$\delta(\eta_*) = \frac{3}{2} \bar{\Phi}_P - 3 [\bar{\Phi}(\eta_*) - \bar{\Phi}_P] = \left(\frac{9}{2} \frac{10}{9} - 3 \right) \bar{\Phi}(\eta_*) = 2 \bar{\Phi}(\eta_*)$$

The relation with the observable temperature that we have looked for is then given by

$$(\Theta_0 + \Psi)(k, \eta_*) = -\frac{1}{6} \delta(k, \eta_*)$$

Hot regions in the temperature map therefore correspond to underdensities in the Dark Matter.

6.3 Acoustic Oscillations

Tight Coupling Limit of the Boltzmann Equations

Not too long before the time η_* (recombination), approximately all of the electrons were ionized, such that the mean free path of a photon is much smaller than the horizon. In other words, Compton scattering caused the electron-proton fluid to be tightly coupled to the photons.

We recall the definition of the optical depth,

$$\tau(\eta) = \int_{-\eta}^{\eta} d\eta' n_e \delta_T a \implies \tilde{v}' = -n_e \delta_T a$$

The light coupling regime corresponds to $\epsilon \gg 1$, and we argue now in more detail, why in this regime the higher multipoles beyond the dipole can be neglected. Recall that the temperature multipoles are given by

$$\Theta_l = \frac{1}{(-i)^l} \int_{-1}^1 \frac{d\mu}{2} P_l(\mu) \Theta(\mu)$$

as well as the Boltzmann equation for photons

$$(\Theta)' + ik_\mu (\Theta) = -\Phi' - ik_\mu \Psi - T' \left[\Theta_0 - \Theta + \mu v_b - \frac{1}{2} P_2(\mu) \Pi \right]$$

Now, we take moments by multiplying with P_l (we take $l > 2$) and find (neglecting Π)

$$(\Theta_l)' + \frac{k}{(-i)^{l+1}} \int_{-1}^1 \frac{d\mu}{2} \mu P_l(\mu) \Theta(\mu) = \tilde{v}' \Theta_l$$

Making use of the recurrence relation

$$(l+1)P_{l+1}(\mu) = (2l+1)\mu P_l(\mu) - l P_{l-1}(\mu)$$

we can perform the integral, such that

$$(\Theta_l)' - \frac{k l}{2l+1} \Theta_{l-1} + \frac{k(l+1)}{2l+1} \Theta_{l+1} = \tilde{v}' \Theta_l$$

The first term on the left is of order $\frac{1}{\eta} \Theta_l$, while the term on the right is of order $\frac{\tilde{v}}{\eta} \Theta_l$. We therefore neglect the term $(\Theta_l)'$ and ignore the term with Θ_{l+1} for now. It follows that

$\Theta_l \sim \frac{k\eta}{2\tilde{v}} \Theta_{l-1}$ and hence $\Theta_l \ll \Theta_{l-1}$ for horizon-size modes ($k\eta \approx 1$). This relation also justifies ignoring the Θ_{l+1} term. All modes higher than the dipole are therefore small compared to monopole and dipole.

Physically, this means that the last scattering surface is much closer to the observer than the wavelength of the mode, such that Compton scattering effectively isotropises the photons.

We should also note that short-wavelength modes with $k \gamma \sim \tilde{v}$ are suppressed due to photon diffusion damping, such that we only need to consider the monopole and the dipole on all scales during the tight coupling regime. Now, we look at the first two moments, which are when neglecting Θ_2 :

$$\Theta'_0 + k \Theta_1 = -\bar{\Psi}'$$

$$\Theta'_1 - \frac{k}{3} \Theta_0 = k \frac{4}{3} + \tilde{v}' \left[\Theta_1 - \frac{i}{3} v_b \right]$$

These are to be combined with the Boltzmann equations

$$v_b' + ik v_b = -3 \bar{\Psi}'$$

$$v_b' + \frac{a'}{a} v_b = -ik \bar{\Psi} + \frac{\tilde{v}'}{R} [v_b + 3i \Theta_1] \text{ where } \frac{1}{R} = \frac{4 C_B^{(0)}}{3 C_B^{(0)}}$$

We put the latter equation into the form

$$v_b = -3i \Theta_1 + \frac{R}{\tilde{v}'} \left[v_b' + \frac{a'}{a} v_b + ik \bar{\Psi} \right]$$

Therefore, to lowest order, $v_b = -3i \Theta_1$. We substitute this into the second term and find

$$v_b = -3i \Theta_1 + \frac{R}{\tilde{v}'} \left[-3i \Theta_1' - 3i \frac{a'}{a} \Theta_1 + ik \bar{\Psi} \right]$$

We can now eliminate v_b from the equation for Θ_1 :

$$\Theta_1' + \frac{a'}{a} \frac{R}{1+R} \Theta_1 - \frac{k}{3(1+R)} \Theta_0 = k \frac{4}{3}$$

Now we differentiate the zeroth moment equation and

substitute $\dot{\phi}_1'$ such that

$$\dot{\phi}_0'' + k \left[\frac{k\psi}{3} - \frac{a'}{a} \frac{R}{1+R} \dot{\phi}_1 + \frac{k}{3(1+R)} \dot{\phi}_0 \right] = -\dot{\Phi}''$$

To eliminate $\dot{\phi}_1$, we use the zeroth moment equation once more with the result

$$\dot{\phi}_0'' + \frac{a'}{a} \frac{R}{1+R} \dot{\phi}_0' + k^2 c_s^2 \dot{\phi}_0 = -\frac{k^2}{3} \psi - \frac{a'}{a} \frac{R}{1+R} \dot{\Phi}' - \dot{\Phi}'' =: F(k, \eta)$$

We have defined here the forcing function F as the right-hand-side terms and the sound speed of the fluid as

$$c_s = \sqrt{\frac{1}{3(1+R)}}$$

The sound speed depends on the baryon density and reduces to the standard value $c_s = \frac{1}{\sqrt{3}}$ for a relativistic fluid in the absence of baryons.

It can also be useful to recast above equation as

$$\left[\frac{\partial^2}{\partial \eta^2} + \frac{R'}{1+R} \frac{\partial}{\partial \eta} + k^2 c_s^2 \right] (\dot{\phi}_0 + \dot{\Phi}) = \frac{k^2}{3} \left(\frac{1}{1+R} \dot{\Phi} - \psi \right)$$

where we have used that $R \propto a \Rightarrow \frac{a'}{a} = \frac{R'}{R}$.

Tightly Coupled Solutions

The Hubble damping term is of order $\frac{1}{\eta^2} \frac{R}{1+R}$, i.e. inside the horizon, where $k\eta \gg 1$, it is negligible compared to the pressure term. The same is true deep in the radiation-dominated regime, where $R \ll 1$. To gain analytic insight, we therefore neglect Hubble damping for now.

We account for a possible time-dependence of c_s and define the sound horizon

$$\tau_s(\eta) = \int_0^\eta dy' c_s(y')$$

Then, $G(\eta, \eta') = \frac{1}{k c_s(\eta)} \partial(\eta - \eta') \sin(k\tau_s(\eta) - k\tau_s(\eta'))$ is the retarded Green function for above equation.

Adding the general homogeneous solutions, we find

$$\Theta_0(\eta) + \Phi(\eta) = C_1 \sin(k\tau_s(\eta)) + C_2 \cos(k\tau_s(\eta))$$

$$+ \frac{k}{3c_s} \int_0^\eta dy' [\Phi(\eta') - \Psi(\eta')] \sin(k\tau_s(\eta) - k\tau_s(\eta'))$$

As we found as a initial condition that $\Theta_0 + \Phi = \text{const.}$, it should be $C_1 = 0$ and $C_2 = \Theta_0(0) + \Phi(0)$. Setting after all $c_s = \frac{1}{\sqrt{3}}$, we obtain

$$\Theta_0(\eta) + \Phi(\eta) = [\Theta_0(0) + \Phi(0)] \cos(k\tau_s(\eta))$$

$$+ \frac{k}{\sqrt{3}} \int_0^\eta dy' [\Phi(\eta') - \Psi(\eta')] \sin(k\tau_s(\eta) - k\tau_s(\eta'))$$

The plot shows (dashed) the present solution compared to those including diffusion damping that we treat below.

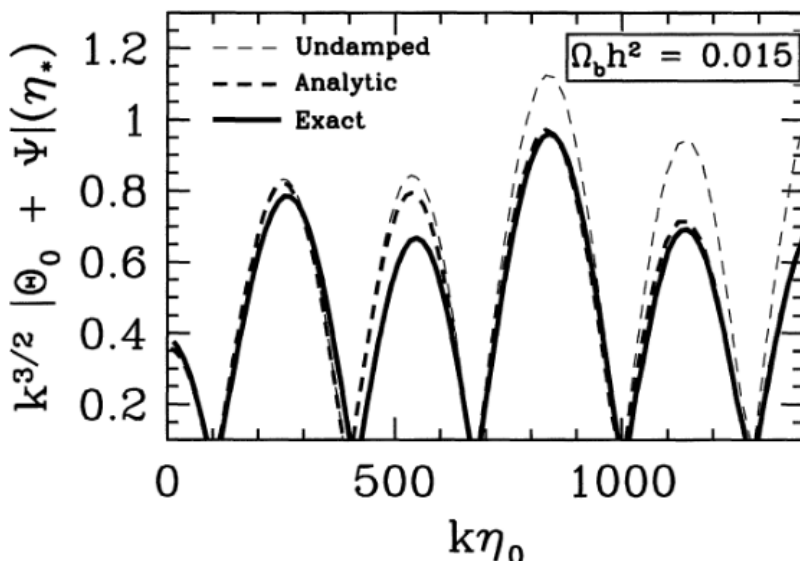


Figure 8.6. The monopole at recombination in a standard CDM model. The exact solution is the heavily weighted solid line. The light dashed line is the undamped solution of Section 8.3, Eq. (8.24); the heavier curve in the middle accounts for damping using the treatment of Section 8.4.

The following interesting points can already be spelt

out at the present level of approximations:

- Peaks appear for $k = \frac{n\pi}{r_s}$, $n=1, 2, \dots$

- It is a useful approximation to divide the problem into a calculation of the gravitational potentials generated by Dark Matter and the effect of these potentials on the temperature anisotropies.

Now, we differentiate the above solution and use that

$$\Theta_0' + \bar{\Phi}' = -k\Theta_0, \text{ such that we obtain}$$

$$\begin{aligned} \Theta_1(\eta) &= \frac{1}{\sqrt{3}} [\Theta_0 + \bar{\Phi}(0)] \sin(kr_s) \\ &\quad - \frac{k}{3} \int_0^\eta d\eta' [\bar{\Phi}(\eta') - \Psi(\eta')] \cos(kr_s(\eta) - kr_s(\eta')) \end{aligned}$$

where we note a phase mismatch with the monopole term.

6.4 Diffusion Damping

Diffusion occurs due to the quadrupole, that is small but at late times non-negligible. It affects only small scales that enter already during radiation domination. We can therefore neglect the gravitational potentials, that are highly suppressed for these modes.

Extending the moment expansion of

$$\Theta' + ik_\mu \Theta = -\bar{\Phi}' - ik_\mu \Psi - \bar{\sigma}' [\Theta_0 - \Theta + \mu v_b - \frac{1}{2} P_2(\mu) \bar{\Pi}]$$

up to the $\ell=2$ mode, and dropping $\bar{\Phi}, \Psi$, we find

$$\Theta_0' + k \Theta_1 = 0$$

$$\Theta_1' + k \left(\frac{2}{3} \Theta_2 - \frac{1}{3} \Theta_0 \right) = \bar{\sigma}' \left(\Theta_1 - i \frac{v_b}{3} \right)$$

$$\Theta_2' - \frac{2}{5} k \Theta_1 = \frac{9}{10} \bar{\sigma}' \Theta_2$$

where we have used $P_2(\mu) = \frac{1}{2} (3x^2 - 1)$ and $\bar{\Pi} = \Theta_2 + \underbrace{\Theta_{P_2} + \Theta_{P_0}}_{\text{neglect}}$,

$$-\int \frac{d\mu}{2} P_2(\mu) = -\frac{1}{5}$$

and above relation (in which Π is neglected)

$$\Theta'_l - \frac{kl}{2l+1} \Theta_{l-1} + \frac{k(l+1)}{2l+1} \Theta_{l+1} = \tilde{\tau}' \Theta_l$$

Also neglecting Ψ , we supplement the network of equations with the velocity equation

$$3i \Theta_1 + v_b = \frac{R}{\tau'} \left[v_b' + \frac{a'}{a} v_b \right]$$

We express the time dependence of the velocity as

$$v_b \propto e^{i\omega dy}$$

Due to tight coupling, $\text{Re}[\omega] \approx k \text{cs}$, while damping should be described through the imaginary part.

Since damping occurs on small scales, i.e. it affects the modes that oscillate more rapidly, we can make use of the relation

$$v_b' = i\omega v_b \gg \frac{a'}{a} v_b$$

since $\frac{a'}{a}$ is of order η whereas ω is of order k .

Consequently, we neglect the second term in the square brackets of the velocity equations, which then becomes

$$v_b = -3i \Theta_1 + \frac{R}{\tau'} i\omega v_b \Rightarrow$$

$$v_b = -3i \Theta_1 \left(1 - \frac{i\omega R}{\tau'} \right)^{-1} \approx -3i \Theta_1 \left[1 + \frac{i\omega R}{\tau'} - \left(\frac{i\omega R}{\tau'} \right)^2 \right]$$

In the quadrupole equation, we neglect Θ'_2 compared to $\tilde{\tau}' \Theta_2$, leaving

$$\Theta_2 = -\frac{4}{9} \frac{k}{\tau'} \Theta_1$$

This again reflects the suppression of the quadrupole compared to the dipole.

The monopole equation gives us

$$i\omega \Theta_0 = -k \Theta_1$$

Inserting back into the dipole equation and dividing by Θ_1 gives us the dispersion relation for sound waves

$$i\omega - \frac{8}{27} \frac{k^2}{\tilde{\epsilon}'} - \frac{i}{3} \frac{k^2}{\omega} = \tilde{\epsilon}' \left[-\frac{i\omega R}{\tilde{\epsilon}'} + \left(\frac{\omega R}{\tilde{\epsilon}'} \right)^2 \right]$$

\Rightarrow

$$\omega^2 (1+R) - \frac{k^2}{3} + \frac{i\omega}{\tilde{\epsilon}'} \left[\omega^2 R^2 + \frac{8k^2}{27} \right] = 0$$

The leading terms in the $\frac{1}{\tilde{\epsilon}'}$ expansion recover that the frequency equals the wave number times the speed of sound. Substituting this zeroth order solution back into the $\frac{1}{\tilde{\epsilon}'}$ terms gives us the first order correction: ($\omega^2 = \omega^{(0)2} + 2\omega^{(0)}\delta\omega + \dots$)

$$\delta\omega = \frac{ik^2}{2(1+R)\tilde{\epsilon}'} \left[c_s^2 R^2 + \frac{8}{27} \right]$$

The perturbations therefore evolve according to damped oscillations

$$\Theta_0, \Theta_1 \sim e^{ik \int_0^\eta dy' c_s} e^{-\frac{k^2}{k_D^2}}$$

recall:

where we define the damping wave number $\tilde{\epsilon}' = -n_e \bar{\sigma}_T a$

$$\frac{1}{k_D^2(\eta)} = \int_0^\eta \frac{dy'}{6(1+R)n_e \bar{\sigma}_T a(\eta')} \left(\frac{R^2}{1+R} + \frac{8}{9} \right)$$

$$c_s = \sqrt{\frac{1}{3(1+R)}}$$

In short, and less accurately, we can say that the damping wave number scales as

$$\frac{1}{k_D} \sim \sqrt{\frac{n}{n_e \bar{\sigma}_T a}}$$

in agreement with the qualitative estimate based on

random walk arguments at the beginning of this Chapter.

6.5 Inhomogeneities to Anisotropies

We now aim for a relation between the photon multipole today, $\Theta_\ell(\eta_0)$ with the monopole and the dipole at recombination.

For this purpose, we first subtract $\tilde{\epsilon}' \Theta$ from $\Theta' + ik_\mu \Theta = -\tilde{\Phi}' - ik_\mu \Psi - \tilde{\epsilon}' [\Theta_0 - \Theta + \mu v_b - \frac{1}{2} P_2(\mu) \Pi]$, such that we can write

$$\Theta' + (ik_\mu - \tilde{\epsilon}') \Theta = e^{-ik_\mu \eta + \tilde{\epsilon}} \frac{d}{d\eta} [\Theta e^{ik_\mu \eta - \tilde{\epsilon}}] = \tilde{S}$$

where

$$\tilde{S} = -\tilde{\Phi}' - ik_\mu \Psi - \tilde{\epsilon}' [\Theta_0 + \mu v_b - \frac{1}{2} P_2(\mu) \Pi]$$

Now we multiply both sides of this equation with $e^{ik_\mu \eta - \tilde{\epsilon}}$ and integrate over η , to obtain

$$\Theta(\eta_0) = \Theta(\eta_{\text{init}}) e^{ik_\mu (\eta_{\text{init}} - \eta_0)} e^{-\tilde{\epsilon}(\eta_{\text{init}})} + \int_{\eta_{\text{init}}}^{\eta_0} d\eta \tilde{S}(\eta) e^{ik_\mu (\eta - \eta_0) - \tilde{\epsilon}(\eta)}$$

Note here that $\tilde{\epsilon}(\eta_0) = 0$ by definition.

Anisotropies present at early times will be erased effectively, what is reflected by the fact that $\tilde{\epsilon}(\eta)$ becomes very large for $\eta \rightarrow 0$. We can therefore set $\eta_{\text{init}} = 0$ and find

$$\Theta(k_\mu, \eta_0) = \int_0^{\eta_0} d\eta \tilde{S}(k_\mu, \eta) e^{ik_\mu (\eta - \eta_0) - \tilde{\epsilon}(\eta)}$$

Now we once again take moments, i.e. we multiply with $P_l(\mu)$ and then integrate $\int_{-1}^1 \frac{d\mu}{2}$. The left-hand side gives $(-i)^l \Theta_\ell$.

Concerning the right-hand side, note that the μ -independent contributions yield

$$\int_{-\infty}^{\infty} \frac{d\mu}{2} P_\ell(\mu) e^{ik\mu(y-y_0)} = \frac{1}{(-i)\ell} j_\ell(k(y-y_0))$$

The μ -dependent terms in \tilde{S} are dealt with by partial integration, for example

$$\begin{aligned} -ik \int_0^{y_0} dy \mu \Psi e^{ik\mu(y-y_0) - \tilde{\tau}(y)} &= - \int_0^{y_0} dy \Psi e^{-\tilde{\tau}(y)} \frac{d}{dy} e^{ik\mu(y-y_0)} \\ &= \int_0^{y_0} dy e^{ik\mu(y-y_0)} \frac{d}{dy} [\Psi e^{-\tilde{\tau}(y)}] \end{aligned}$$

The boundary terms at $y=0$ vanish because $\tilde{\tau}(y)$ is very large there. At $y=y_0$, there is no angular dependence. These terms therefore only lead to an indetectable change in the monopole and are hence dropped here.

Proceeding similarly for the other terms in \tilde{S} , we obtain

$$\Theta_\ell(k, y_0) = \int_0^{y_0} dy S(k, y) j_\ell(k(y_0 - y))$$

where

$$\begin{aligned} S(k, y) &= e^{-\tilde{\tau}(y)} \left[-\tilde{\Phi}' - \tilde{\tau}' \left(\Theta_0 + \frac{1}{4}\pi \right) \right] + \frac{d}{dy} \left[e^{-\tilde{\tau}(y)} \left(\Psi + \frac{iV_6 \tilde{\tau}(y)}{k} \right) \right] \\ &\quad - \frac{3}{4k^2} \frac{d^2}{dy^2} \left(e^{-\tilde{\tau}(y)} \tilde{\tau}'(y) \pi \right) \end{aligned}$$

We have used here also the property $j_\ell(x) = (-1)^\ell j_\ell(-x)$.

Now, we introduce the visibility function

$$g(y) = -\tilde{\tau}' e^{-\tilde{\tau}}$$

that has the property

$$\int_0^{y_0} dy g(y) = \int_0^{y_0} dy \frac{d}{dy} e^{-\tilde{\tau}} = 1$$

and that can apparently be interpreted as the probability that a photon was last scattered between the times y and $y+dy$. It should go to zero for $y \rightarrow \infty$ as well as for $y \rightarrow 0$.

and peak around recombination.

Neglecting the polarisation tensor Π that only yields a small contribution, we can express the source in terms of the visibility function as

$$S(k, \eta) \approx g(\eta) [\Theta_0(k, \eta) + \Psi(k, \eta)] + \frac{d}{d\eta} \left(\frac{i v_b(k, \eta) g(\eta)}{k} \right) + e^{-\tau(\eta)} [\Psi'(k, \eta) - \bar{\Phi}'(k, \eta)]$$

We substitute this into the equation for the multipole moments, integrate the term involving v_b by parts and obtain

$$\begin{aligned} \Theta_\ell(k, \eta_0) = & \int_0^{\eta_0} d\eta \, g(\eta) [\Theta_0(k, \eta) + \Psi(k, \eta)] j_\ell(k(\eta_0 - \eta)) \\ & - \int_0^{\eta_0} d\eta \, g(\eta) \frac{i v_b(k, \eta)}{k} \frac{d}{d\eta} j_\ell(k(\eta_0 - \eta)) \\ & + \int_0^{\eta_0} d\eta \, e^{-\tau} [\Psi'(k, \eta) - \bar{\Phi}'(k, \eta)] j_\ell(k(\eta_0 - \eta)) \end{aligned}$$

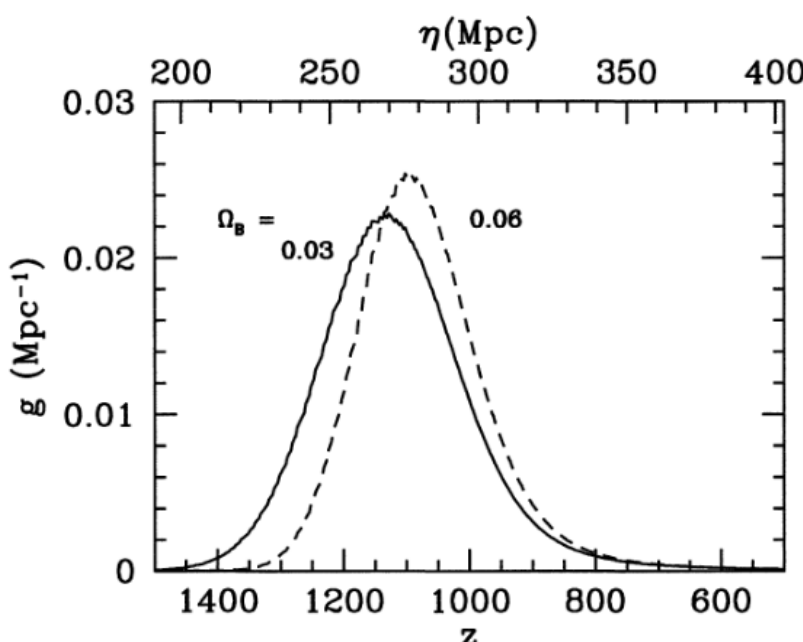


Figure 8.9. The visibility function. Most electrons last scatter at around $z \approx 1100$ with little dependence on the baryon density. Note that the integral of g over conformal time is 1. Here $h = 0.5$.

We observe terms weighted by $e^{-\tau}$ and by the visibility function. The $e^{-\tau}$ terms contribute for $\tau \lesssim 1$, i.e. after recombination and account for the gravitational redshift.

blue shift from changing gravitational potentials, which is referred to as the integrated Sachs-Wolfe effect. Regarding the first two terms, the visibility function is so sharply peaked around recombination such that the remaining factors in the integrand may be approximated as constants. We furthermore replace the derivative term using the fact that

$$\frac{d j_l}{dx} = j_{l-1} - \frac{l+1}{x} j_l$$

and the above approximate relation $v_b \approx -3i\Theta_1$. We then arrive at

$$\begin{aligned} \Theta_l(k, \eta_0) &\approx [\Theta_0(k, \eta_*) + 4(k, \eta_*)] j_l(k(\eta_0 - \eta_*)) \\ &+ 3\Theta_1(k, \eta) \left[j_{l-1}(k(\eta_0 - \eta_*)) - \frac{l+1}{k(\eta_0 - \eta_*)} j_l(k(\eta_0 - \eta_*)) \right] \\ &+ \int_0^{\eta_0} d\eta e^{-\tau} [\Psi'(k, \eta) - \Phi'(k, \eta)] j_l(k(\eta_0 - \eta)) \end{aligned}$$

The temperature field of the CMB is observed on a sphere at a fixed distance from the present observers. We recall that we expressed the temperature as

$$T(\vec{x}, \vec{p}, \eta) = T(\eta) [1 + \Theta(\vec{x}, \vec{p}, \eta)].$$

We can only observe this at (η_0, \vec{x}_0) , such that the remaining handle is the photon direction \vec{p} . We therefore use the standard decomposition in terms of spherical harmonics

$$\Theta(\vec{x}, \vec{p}, \eta) = \sum_{l=1}^{\infty} \sum_{m=-l}^l a_{lm}(\vec{x}, \eta) Y_{lm}(\vec{p})$$

Making use of the orthonormality relation

$$\int d\Omega Y_{lm}(\vec{p}) Y_{l'm'}^*(\vec{p}) = \delta_{ll'} \delta_{mm'}$$

we can invert above relation to obtain

$$a_{lm}(\vec{x}, \eta) = \int \frac{d^3k}{(2\pi)^3} e^{i\vec{k} \cdot \vec{x}} \int d\Omega Y_{lm}^*(\vec{p}) \mathcal{D}(\vec{k}, \vec{p}, \eta)$$

Hence, we can use the $a_{lm} \equiv a_{lm}(\vec{x}_0, \eta_0)$ as the observables. Due to the stochastic nature of the initial conditions, there are no predictions for the values of the a_{lm} , but only of their variance, what defines the C_l :

$$\langle a_{lm} \rangle = 0, \quad \langle a_{lm} a_{l'm'}^* \rangle = \delta_{ll'} \delta_{mm'} C_l.$$

The C_l are "measured" by sampling over the $2l+1$ values of m . Hence, the accuracy of the observation is statistically limited as characterised by the uncertainty

$$\left(\frac{\Delta C_l}{C_l} \right) = \sqrt{\frac{2}{2l+1}}$$

which is called cosmic variance. Of course, additional uncertainties may arise from foregrounds and the instrument's resolution.

Earlier in this Chapter, we have computed the temperature perturbation in a given gravitational potential. We recall that at late times, the Poisson equation relates these to the matter overdensity δ as

$$\delta(\vec{k}, a) = \frac{k^2 \Phi(\vec{k}, a)}{\frac{3}{2} \Omega_m H_0^2}$$

This implies, we can use the results of this Chapter to compute $\frac{\mathcal{D}(\vec{k}, \beta)}{\delta(\vec{k})}$ and use the prediction for the matter power spectrum $P(k)$ to obtain the temperature anisotropy observed today. We hence express

$$\begin{aligned} \langle \Theta(\vec{k}, \vec{p}) \Theta^*(\vec{k}', \vec{p}') \rangle &= \langle \delta(\vec{k}) \delta^*(\vec{k}') \rangle \frac{\Theta(\vec{k}, \vec{p})}{\delta(\vec{k})} \frac{\Theta^*(\vec{k}', \vec{p}')}{\delta(\vec{k}')} \\ &= (2\pi)^3 \delta(\vec{k} - \vec{k}') P(\vec{k}) \frac{\Theta(\vec{k}, \vec{k} \cdot \vec{p})}{\delta(\vec{k})} \frac{\Theta^*(\vec{k}', \vec{k}' \cdot \vec{p}')}{\delta(\vec{k}')} \end{aligned}$$

where we drop the arguments \vec{q}_0 . Then,

$$\begin{aligned} C_\ell &= \int \frac{d^3 k}{(2\pi)^3} \frac{d^3 k'}{(2\pi)^3} e^{i(\vec{k} - \vec{k}') \cdot \vec{x}} \int d\Omega d\Omega' Y_{\ell m}^*(\vec{p}) Y_{\ell m}(\vec{p}') \\ &\quad * \langle \Theta(\vec{k}, \vec{p}) \Theta^*(\vec{k}', \vec{p}') \rangle \\ &= \int \frac{d^3 k}{(2\pi)^3} P(k) \int d\Omega Y_{\ell m}^*(\vec{p}) \frac{\Theta(\vec{k}, \vec{k} \cdot \vec{p})}{\delta(\vec{k})} \int d\Omega' Y_{\ell m}(\vec{p}') \frac{\Theta^*(\vec{k}', \vec{k}' \cdot \vec{p}')}{\delta(\vec{k}')} \\ &= \int \frac{d^3 k}{(2\pi)^3} P(k) \sum_{\ell' \ell''} (-i)^{\ell' \ell''} (2\ell' + 1) (2\ell'' + 1) \frac{\Theta_{\ell'}(\vec{k}) \Theta_{\ell''}^*(\vec{k})}{|\delta(\vec{k})|^2} \\ &\quad * \int d\Omega P_{\ell'}(\vec{k} \cdot \vec{p}) Y_{\ell m}^*(\vec{p}) \int d\Omega' P_{\ell''}(\vec{k}' \cdot \vec{p}') Y_{\ell m}(\vec{p}') \\ &= \int \frac{d^3 k}{(2\pi)^3} P(k) \sum_{\ell' \ell''} (-i)^{\ell' \ell''} (2\ell' + 1) (2\ell'' + 1) \frac{\Theta_{\ell'}(\vec{k}) \Theta_{\ell''}^*(\vec{k})}{|\delta(\vec{k})|^2} \\ &\quad * \frac{16\pi^2}{(2\ell + 1)^2} |Y_{\ell m}(\vec{k})|^2 \delta_{\ell \ell'} \delta_{\ell \ell''} \\ &= \frac{2}{\pi} \int_0^\infty k^2 dk P(k) \frac{|\Theta_\ell(\vec{k})|^2}{|\delta(\vec{k})|^2} \end{aligned}$$

We have used here in the second step that

$$\Theta(\vec{k}, \vec{k} \cdot \vec{p}) = \sum_l (-i)^l (2\ell + 1) P_\ell(\vec{k} \cdot \vec{p}) \Theta_\ell(\vec{k})$$

and for the third step

$$\begin{aligned} \int d\Omega Y_{\ell m}(\vec{p}) P_{\ell'}(\vec{p} \cdot \vec{k}) &= \int d\Omega Y_{\ell m}(\vec{p}) \frac{4\pi}{2\ell + 1} \sum_{m'} Y_{\ell m'}^*(\vec{p}) Y_{\ell' m'}(\vec{k}) \\ &= \frac{4\pi}{2\ell + 1} \delta_{\ell \ell'} Y_{\ell' m'}(\vec{k}) \end{aligned}$$

6.6 The CMB Observed Today

First consider very large scales, i.e. $k\eta_* \lesssim 1$. There is no causal contact and hence no dipole develops, and $\bar{\Phi}(k) \approx \frac{g}{10} \bar{\Phi}_P(k)$ is frozen, up to the late-time behaviour described by the growth function. Only the first term in the expression for $\bar{\Psi}_Q(k, \eta_0)$ therefore contributes.

Using the large scale relation $\bar{\Psi} + \Psi \approx \frac{1}{3} \Psi$, neglecting anisotropic stress, $\bar{\Phi} = -\Psi$ and the Poisson equation, we then obtain

$$\begin{aligned}\bar{\Psi}_Q(\eta_*) + \Psi(\eta_*) &\approx \frac{1}{3D_1(a=1)} \Psi(\eta_0) = -\frac{1}{3D_1(a=1)} \bar{\Phi}(\eta_0) \\ &= -\frac{\Omega_m H_0^2}{2k^2 D_1(a=1)} \delta(\eta_0)\end{aligned}$$

The large l -part of the spectrum, that exhibits no oscillations, is called the Sachs-Wolfe plateau, as we indicate by the subscript SW. Using above results, we obtain

$$C_l^{SW} = \frac{\Omega_m^2 H_0^4}{2\pi D_1^2(a=1)} \int_0^\infty \frac{dk}{k^2} j_l^2(k(\eta_0 - \eta_*)) P(k)$$

Recall that

$$P(k, a) = \frac{g}{25} \frac{k^4}{\Omega_m^2 H_0^4} T^2(k) D_1^2(a) P_{\bar{\Phi}_P}(\vec{k})$$

and the parametrisation

$$\bar{P}_{\bar{\Phi}}(k) = \frac{g}{4} \bar{P}_{\bar{\Phi}_P}(k) = A_S \left(\frac{k}{k_0} \right)^{n_S - 1} = \frac{g}{4} \frac{k^3}{2\pi^2} P_{\bar{\Phi}_P}(k)$$

Hence, setting $T(k) = 1$ on large scales,

$$C_l^{SW} = \frac{8\pi^2}{25} A_S k_0^{-1-n_S} \int_0^\infty dk k^{-2+n_S} j_l^2(k(\eta_0 - \eta_*))$$

$$x = k\eta_0 \quad x = \frac{d\eta}{dx} \quad x = k$$

$$= \frac{8\pi^2}{25} A_S (\eta_0 k_0)^{-1-n_S} \int_0^\infty \frac{dx}{x^{2-n_S}} j_l^2(x)$$

$$= \frac{8\pi^2}{25} A_S (\eta_0 k_0)^{1-n_S} 2^{n-4} \pi \frac{\Gamma(l + \frac{n_S}{2} - \frac{1}{2})}{\Gamma(l + \frac{5}{2} - \frac{n_S}{2})} \frac{\Gamma(3-n_S)}{\Gamma^2(2-\frac{n_S}{2})}$$

For $n_S = 1$, we obtain

$$l(l+1) C_l^{SW} = \frac{4\pi^2}{25} A_S$$

This is the reason why plotting $l(l+1) C_l$, as commonly done, gives a plateau for large l .

For smaller l , the peak positions and the amplitudes of the baryon acoustic oscillations tell tale about the energy composition and the geometry of the Universe, cf. Chapter 1 for an enumeration of the parameters that can be derived.